A Novel N7-Methylguanosine-Related lncRNA Signature Predicts the Prognosis of Colon Adenocarcinoma Patients

Guowei Sun
Dalian Medical University
Yayan Fu
Yangzhou University
Wenzhe Shao
Dalian Medical University
Cangyuan Zhang
Dalian Medical University
Ziyang Long
Dalian Medical University
Li Bao
Yangzhou University
Biao Sun
Yangzhou University
Wei Wang
Dalian Medical University
Liuhua Wang
Northern Jiangsu People's Hospital
Jun Ren
Northern Jiangsu People's Hospital
Qiannan Sun
Northern Jiangsu People's Hospital
Dong Tang
Northern Jiangsu People's Hospital
Daorong Wang (daorong666@sina.com)
Northern Jiangsu People's Hospital

Research Article

Keywords: Bioinformatics analysis, Colon adenocarcinoma, N7-Methylguanosine, lncRNA, prognostic prediction signature

Posted Date: May 13th, 2022

DOI: https://doi.org/10.21203/rs.3.rs-1635343/v1

Abstract

Background: The most common subtype of colorectal cancer is colon adenocarcinoma (COAD). However, few studies have investigated the predictive value of N7-methylguanosine(m7G)-related long-noncoding RNAs (lncRNAs) in COAD. We aim to use m7G-related lncRNAs to construct a prognostic model for COAD.

Methods: RNA-seq data and the corresponding clinical and prognostic Data were downloaded from The Cancer Genome Atlas (TCGA) database.M7G-related lncRNAs with prognostic values were identified using the univariate and multivariate Cox regression. Based on Kaplan-Meier curves, we compared the survival rates in the high-risk and low-risk groups. The functional enrichment of m7G-related lncRNAs with a prognostic value was interpreted using gene set enrichment analysis (GSEA). Finally, we studied the relationship between predictive signature and treatment response in patients with COAD.

Results: Six m7G-related lncRNAs (LINC01063, ARRDC1-AS1, AL354993.2, ZEB1-AS1, SNHG16, LINC02474) were identified to establish a signature. The m7G-related lncRNA signature may be able to predict COAD patients' prognosis independently. The OS times of patients in the high-risk group were shorter than those in the low-risk group. With an area under the receiver operating characteristic curve of 0.742, the m7G-related lncRNA prognostic signature had a better prognostic prediction than clinicopathological variables. The high-risk group has the most tumor-related pathways, according to GSEA. The prognostic characteristic was linked to the immunological state of COAD patients, according to GSEA. The conventional chemotherapy medicines axitinib, cytarabine, sorafenib, parthenolide and vorinostat were more sensitive in high-risk individuals.

Conclusion: Our study develops a COAD risk model consisting of six lncRNAs related to m7G that have independent prognostic values. Clinically, the lncRNA signature could improve prediction of outcomes for patients with COAD and, with further prospective validation, could help guide tailored therapy for COAD patients

Introduction

Colorectal cancer is among the most common cancers worldwide and also one of the top causes of cancer-related deaths[1]. COAD accounts for more than 90% of colorectal malignancies across all clinical subtypes[2]. The current main treatment for COAD includes surgery, radiofrequency ablation, cryosurgery, chemotherapy, radiotherapy, and targeted therapy[3]. Despite recent advances in targeted medicines and immunotherapies, survival rates for COAD patients remain unsatisfactory. The poor results could be attributed to the fact that the majority of the patients were detected late in their disease, making them more likely to develop distant metastases. Patients with locally advanced colon cancer have a 5-year relative survival rate of 90 percent, but those with distant-stage disease have a rate of 14 percent [4]. Given this, it is essential to identify novel biomarkers for predicting prognosis in patients with COAD.

N7-methylguanosine (m7G) is a key RNA cap modification that governs practically every step of mRNA metabolism, including transcription, mRNA splicing, and translation[5]. The N7-methylguanosine (m7G)

cap is added to the beginning of an mRNA and is involved in a variety of important physiological functions, primarily by protecting mRNA from premature cleavage in eukaryotic gene expression. [6]. Even though m7G has been studied for a long time, we still have a limited understanding of its function. Several types of research have indicated that m7G was closely associated with the incidence and progression of malignant tumor types. METTL1/WDR4-mediated m7G tRNA modifications and m7G codon usage promote mRNA translation and lung cancer progression[7]. METTL1-m7G-EGFR/EFEMP1 axis promotes bladder cancer development[8]. METTL1 promotes hepatocarcinogenesis via m7G tRNA modification-dependent translation control[9]. MYC-targeted WDR4 promotes proliferation, metastasis, and sorafenib resistance by inducing CCNB1 translation in hepatocellular carcinoma[10].

Long non-coding RNAs are a class of RNA molecules in eukaryotes that do not encode proteins, have transcripts longer than 200 bp, and can regulate gene expression at multiple levels such as epigenetic regulation, transcriptional regulation, post-transcriptional regulation, etc.[11]. M7G has been shown to be a critical factor in the growth and metastasis of COAD [12, 13]. However, the mechanism by which m7G alteration impacts aberrantly expressed lncRNAs in COAD is unclear, few research has focused on how m7G alteration impacts lncRNAs and thereby contributes to gene regulation. Understanding how m7G-modified lncRNAs contribute to the growth and poor prognosis of COAD will allow researchers to find biomarkers and make therapeutic recommendations.

This study created an m7G-related lncRNA signature; examined its utility in making predictions about the diagnosis, therapy response, and prognosis of COAD patients; and performed internal verification.

Materials And Methods

Data sources and processing

Data on mRNA sequencing, lncRNA sequencing, and corresponding clinical information for 514 patients with COAD were obtained from The Cancer Genome Atlas database (https://portal.gdc.cancer.gov/). The gene expression profiles were quantified by FPKM and normalized through log2-based transformation. Data on disease-free survival (DFS) for 223 COAD patients were downloaded from the cBioPortal database (https://www.cbioportal.org/). 47 m7G-related genes were downloaded from GeneCards (https://www.genecards.org/).

Identification of Prognostic m7G-Related lncRNAs

To mine m7G-related lncRNAs, we used the "limma" R package to calculate the correlation between m7G-related genes and lncRNAs. (with the $|R^2| > 0.3$ and $P<0.001$). Then, we used the "survival" R package to identify m7G-related lncRNAs associated with COAD patients' prognosis via univariate Cox regression analysis. Finally, We constructed the m7G-related lncRNA prediction signature using multivariate Cox regression analysis. The risk score for each patient with COAD was calculated using the formula below in this research:

$$Riskscore = \sum_{i=1}^{n} \left(Coef_i \times x_i \right)$$

Coef indicates the coefficient value, and x indicates selected m7G-related lncRNAs expression levels.

Construction of Nomogram

Using a combination of the signature and clinical factors including stage, sex, age, and N stage, we developed a nomogram that predicts the overall survival of COAD patients at 1, 3, and 5 years. A calibration chart was used to test the accuracy of the prediction, showing the difference between expected and actual survival, with the 45° line indicating the best forecast result.

Functional Enrichment Analysis of the m7G-Related lncRNA Predictive Signature

COAD patients were classified as high-risk and low-risk based on the median risk score. The functional enrichment was interpreted using gene set enrichment analysis (http://www.broad.mit.edu/gsea/)[14]. The statistical significance levels were set at nominal $p < 0.05$ and FDR < 0.25. We used the "GSVA" package to calculate the infiltration scores of 16 immune cells and activity levels of 13 immune-related pathways via single-sample gene set enrichment analysis (ssGSEA)[15].

The Role of the Prognostic Characteristic in Predicting the Clinical Treatment Response

To examine the role of the prognostic characteristic in predicting response to COAD treatment, we calculated the half-maximal inhibitory concentration (IC50) of popular chemotherapeutic drugs used in the clinical treatment of COAD. The Wilcoxon signed-rank test was used to compare the IC50 values between the high- and low-risk groups.

Results

Construction of a Novel Prognostic Risk Signature for COAD

We identified 1041 m7G-related lncRNAs. 37 lncRNAs associated with prognosis were obtained by using univariate Cox regression analysis. 6 lncRNAs associated with 7-methyladenosine (LINC01063, ARRDC1-AS1, AL354993.2, ZEB1-AS1, SNHG16, LINC02474) were identified by multivariate Cox regression analysis and built a predictive signature. Figure 1a shows the expression levels of six m7G-related lncRNAs in COAD patients. We used the "ggalluvial" R software package and Cytoscape to further visualize the lncRNAs. There were 23 pairs of lncRNA-mRNA in the co-expression network (Fig. 1b, $|R2| > 0.4$ and $p < 0.001$). SNHG16 had co-expressive relationship with thirteen 7-methyladenosine-related genes (EIF4E, RNMT, NCBP1, RNGTT, CCNH, GTF2H1, POLR2E, MNAT1, POLR2D, POLR2J, SUPT5H, GTF2H3, IFIT5), ZEB1-AS1 had co-expressive relationship with three m7G-related genes (METTL1,POLR2E,PSMC4), AL354993.2 had co-expressive relationship with three m7G-related genes (POLR2E, CCNH, RNGTT),

ARRDC1-AS1 had co-expressive relationship with two m7G-related genes (POLR2J and DXO), LINC01063 was co-expressed with POLR2D, and LINC02474 was co-expressed with POLR2A. SNHG16 was a protective factor, while LINC02474, LINC01063, ARRDC1-AS1, ZEB1-AS1, and AL354993.2 were risk factors (Fig. 1c). The following formula was used to determine the risk score: risk score=(0.667 × AL354993 expression)+(-1.301 × SNHG16 expression)+(0.531 × LINC02474 expression)+(1.034 × LINC01063 expression)+(0.550 × ARRDC1-AS1 expression)+(0.719 × ZEB1-AS1 expression).

The Correlations Between the prognosis of COAD Patients and the Predictive Signature

Based on the median risk score for each patient, each patient was scored based on the formula, and then grouped into high-risk and low-risk groups. Kaplan Meier analysis was performed on the OS time of the high-risk group and low-risk group to determine the value of the risk score in predicting the prognosis of COAD patients. The OS time of the high-risk group was considerably shorter than that of the low-risk group (Fig. 2a, $p < 0.001$). Figure 2b depicts the risk scores of the high- and low-risk groups. As the risk score increased, more and more patients died (Fig. 2c). We used Cox regression analysis to determine if the predictive signature is an independent prognostic factor for COAD patients. Stage, T stage, M stage, N stage, and risk score were all found to be substantially linked with COAD patients' overall survival in a univariate Cox regression analysis (Fig. 2d). Risk scores and age were found to be independent predictors of OS in COAD patients in multivariate Cox regression analysis (Fig. 2e, $p < 0.05$). The risk score's AUC was 0.742, which was higher than clinicopathological factors when it came to predicting COAD patients' prognosis (Fig. 2f). The AUCs of 1, 3, and 5-years survival were 0.707, 0.763, and 0.790, respectively, which indicated good predictive performance (Fig. 2g).

We created a nomogram with clinicopathological factors and the risk score to better predict the OS of COAD patients at 1, 3, and 5 years (Figs. 3b-d). The calibration chart showed the best prediction accuracy, and the predicted survival rates were approximately equal to the actual survival rates.

Internal Validation of the Predictive Signature

To assess the applicability of the prediction signature for OS based on the entire TCGA dataset, we randomly divided the 417 COAD patients into two cohorts ($n1 = 209$, $n2 = 208$). In the first internal cohort, the OS rate of patients in the high-risk group was lower than that of the low-risk group (Fig. 4a, $p < 0.001$), which was similar to the results seen across the entire dataset. In the second internal cohort, the high-risk group's prognosis was worse than the low-risk group's (Fig. 4b, $p < 0.001$). The ROC curves of the two cohorts showed excellent prediction performance. ROC curve analysis gave acceptable AUC values of 0.757, 0.767, and 0.873 for 1-year, 3-year, and 5-year survival, respectively, in the first internal cohort. ROC curve analysis gave acceptable AUC values of 0.647, 0.763, and 0.728 for 1-year, 3-year, and 5-year survival, respectively, in the second internal cohort.

Gene Enrichment Analysis and Immune Cell Infiltration

We used GSEA to study the differences between high-risk and low-risk groups. We investigated that snare inter, in vesicular transport, citrate cycle traction cycle, and gluconeogenesis were significantly enriched in the high-risk group (Supplementary tableS1). We explored the correlation between risk scores and immune cells and immune functions by calculating ssGSEA enrichment scores for different immune cell subpopulations, related functions, or pathways. The results showed that the high-risk group had significantly higher levels of helper T-cell type 1 (Th1) cells than the low-risk group (Supplementary FigureS1a). In addition, the immune function scores of T-cell co-inhibition and T-cell co-stimulation were higher in the high-risk group than in the low-risk group (Supplementary FigureS1b). The above results suggest that the immune function may be more active in the high-risk group.

Correlation Between the Predictive Signature and COAD Therapy

We explored the relationship between predictive models of COAD and the efficacy of conventional chemotherapy. The results revealed that the IC50s of axitinib, cytarabine, sorafenib, parthenolide, and vorinostat were greater in the high-risk group, whereas the IC50 of lapatinib was lower (Figs. 5a–f), which is useful for developing customized treatment plans for patients in the high- and low-risk groups.

Construction of the m7G-Related lncRNA Predictive Signature for DFS

Given the importance of DFS in COAD patients' prognosis, we created an m7G-related lncRNA predictive signature for DFS. A total of 177 COAD patients' DFS data were gathered from the cBioPortal database. Five N7-methylguanosine-related lncRNAs were revealed to be substantially correlated with DFS in COAD patients after univariate Cox regression analysis. Three m7G-related lncRNAs were found after multivariate Cox regression analysis to generate the prediction signature. Risk score = (-2.593 SNHG16) + (-1.752 LINC01871)+(1.359 AC132192.2). According to the algorithm, each patient's risk score was computed, and the patients in the overall dataset were separated into two groups based on the median value: high-risk and low-risk. The DFS of the high-risk group was considerably shorter than that of the low-risk group (Fig. 6a, $p<0.01$), according to a Kaplan-Meier survival curve analysis. The AUCs of 1, 3, and 5- years survival were 0.765, 0.814, and 0.923, respectively (Fig. 6d).

To test the sensitivity and specificity of predictive signature for DFS, we randomized 177 patients into two groups: the first internal cohort (n = 89) and the second internal cohort (n = 88). The median value was used to separate patients into high- and low-risk groups, and the results throughout the full dataset were consistent. The DFS of patients in the high-risk group was shorter in the first internal cohort (Fig. 6b, $p<0.01$) and the second internal cohort (Fig. 6c, $p<0.01$) compared to the low-risk group. The AUCs for 1, 3, and 5-year survival in the first internal cohort were 0.918, 0.899, and 1.000, respectively (Fig. 6e). The AUCs for 1, 3, and 5-year survival in the second internal cohort were 0.627, 0.821, and 0.868, respectively (Fig. 6f).

Discussion

COAD is one of the most frequent malignant tumors of the digestive tract, with the majority of cases stemming from colorectal epithelial cells. The role of m7G in cancer is complicated. The involvement of m7G in the formation and progression of cancer has been discovered in a growing number of studies, although there are few investigations on its significance in cancer prognosis. It has not been reported that building an m7G-related lncRNA prediction signature can predict the prognosis of COAD patients.

lncRNAs have been demonstrated to play a crucial role in COAD in numerous studies. As a result, identifying an m7G-related lncRNA prediction characteristic in COAD patients is critical.

In this study, we used univariate Cox regression analysis to obtain 37 lncRNAs associated with the prognosis of COAD patients. Then, six m7 G-related lncRNAs (LINC01063, ARRDC1-AS1, AL354993.2, ZEB1-AS1, SNHG16, LINC02474) were obtained by multivariate Cox regression analysis to construct the prognosis model. Five m7G-related lncRNAs (LINC01063, ARRDC1-AS1, AL354993.2, ZEB1-AS1, SNHG16, and LINC02474) were reported to be associated with cancer. In melanoma, LINC01063 acts as an oncogene by regulating SOX12 expression via the miR-5194 pathway[16]. STAT1 activates the long noncoding RNA ARRDC1-AS1, which has oncogenic characteristics in glioma through sponging the miR-432-5p/PRMT5 axis[17]. lncRNA ZEB1-AS1Positive Reciprocal Feedback of and α Contributes to Hypoxia-Promoted Tumorigenesis and Metastasis of Pancreatic Cancer[18]. In human gastric cancer, SNHG16 lncRNAs are overexpressed and may be carcinogenic via influencing cell cycle progression[19]. Long noncoding RNA LINC02474 affects colorectal cancer metastasis and apoptosis by inhibiting GZMB expression[20]. We also found mRNA (DXO, EIF4E, RNMT, NCBP1, RNGTT, CCNH, GTF2H1, POLR2A, POLR2D, POLR2E, POLR2J, PSMC4, METTL1, MNAT1, SUPT5H, GTF2H3, and IFIT5) significantly co-expressed with these lncRNAs. Among them, by preventing DXO destabilization of cyclin D1 mRNA, NPL4 upregulation increases bladder cancer cell proliferation[21]. Upregulation of the eukaryotic translation initiation factor 4E is linked to a poor prognosis in gallbladder cancer patients and enhances cell proliferation both in vitro and in vivo[22]. The interaction between the methyl-7-guanosine cap maturation enzyme RNMT and the cap-binding protein eIF4E has been identified and characterized[23]. Through up-regulation of CUL4B, NCBP1 promotes the progression of lung adenocarcinoma[24]. As a carcinoma inducer, cyclin H regulates lung cancer progression[25]. POLR2A promotes gastric cancer cell proliferation by advancing cell cycle progression overall[26]. SUPT5H post-transcriptional silencing modulates PIN1 expression in human breast cancer cells, inhibits tumorigenicity, and induces apoptosis[27]. Micro-RNA378a-3p induces apoptosis in sarcomatoid renal cell carcinoma and regulates POLR2A and RUNX2 expression[28]. The roles and mechanism of IFIT5 in bladder cancer epithelial-mesenchymal transition and progression[29].

We calculated the risk score for each patient using the formula. According to the median value, the patients were separated into high-risk and low-risk groups. The OS of the high-risk group was shorter than the low-risk group. The predictive signature has a strong predictive performance, according to the ROC curve. In predicting the prognosis of COAD patients, the predictive signature was more reliable than clinicopathological factors. The predictive signature has strong predictive performance, according to internal verification.

GSEA showed that compared with the low group, the high-risk group was mainly enriched in snare interactions in vesicular transport, citrate cycle TCA cycle and gluconeogenesis. The literature suggests that high PLOD3 expression in COAD leads to a poor prognosis by reducing immune cell infiltration and enhancing tumor-promoting pathways such as gluconeogenesis and TGF-beta signaling in the epithelial-mesenchymal transition (EMT)[30].

We calculated ssGSEA enrichment scores for different immune cell subgroups, immune functions, and pathways to see if there was a link between risk scores and immune cells and functions. The results showed that the T helper type 1 (Th1) cell content was significantly different between the high-risk and low-risk groups and that the immune function scores for T cell co-inhibition and T cell co-stimulation were higher in the high-risk group than in the low-risk group. These findings suggest that the immune system may be more active in the high-risk group. Axitinib, cytarabine, sorafenib, parthenolide, and vorinostat are presumably sensitive to high-risk patients, but they are resistant to lapatinib, according to our findings. This suggests that patients in the high-risk group can obtain better outcomes from immunotherapy combined with chemotherapy, which gives a theoretical foundation for COAD patients to receive tailored treatment.

However, our study has several limits. First, this study just used data from the TCGA database for internal testing; external validation of the predictive signature's applicability still requires data from other databases. Second, to confirm the risk score model's clinical utility, it must be further validated in clinical studies. Furthermore, the functions and mechanisms of the six m7G-related lncRNAs must be investigated further.

To summarize, the m7G-related lncRNA signature can independently predict COAD patients' prognosis. In addition, it can provide the foundation for a putative mechanism of m7G-related lncRNAs in COAD and the efficacy of treatment.

Declarations

Funding

The authors declare that no funds, grants, or other support were received during the preparation of this manuscript.

Competing Interests

The authors have no relevant financial or non-financial interests to disclose.

Author Contributions

Guowei Sun, Daorong Wang, Dong Tang, and Yayan Fu conceived and devised the study. Guowei Sun, Liuhua Wang, Wei Wang, Li Bao, Biao Sun, and Wenzhe Shao performed bioinformatic and statistical analysis. Guowei Sun, Jun Ren, Wei Wang and Cangyuan Zhang found testify data and analysis tools.

Guowei Sun, Qiannan Sun and Ziyang Long supervised research and wrote the manuscript. All authors contributed to the article and approved the submitted version.

Data Availability

The original contributions presented in the study are included in the article/Supplementary Material. Further inquiries can be directed to the corresponding authors.

Ethics approval

Not applicable.

Consent to participate

Not applicable.

Consent to publish

Not applicable.

ACKNOWLEDGMENTS

Thanks to all the peer reviewers and editors for their opinions and suggestions.

References

1. Sung H, Ferlay J, Siegel R, Laversanne M, Soerjomataram I, Jemal A and Bray F (2021) Global Cancer Statistics 2020: GLOBOCAN Estimates of Incidence and Mortality Worldwide for 36 Cancers in 185 Countries. CA: a cancer journal for clinicians 71:209–249. doi: 10.3322/caac.21660
2. Barresi V, Reggiani Bonetti L, Ieni A, Caruso R and Tuccari G (2015) Histological grading in colorectal cancer: new insights and perspectives. Histology and histopathology 30:1059–67. doi: 10.14670/hh-11-633
3. Dekker E, Tanis P, Vleugels J, Kasi P and Wallace M (2019) Colorectal cancer. Lancet (London, England) 394:1467–1480. doi: 10.1016/s0140-6736(19)32319-0
4. Siegel RL, Miller KD, Goding Sauer A, Fedewa SA, Butterly LF, Anderson JC, Cercek A, Smith RA and Jemal A (2020) Colorectal cancer statistics, 2020. CA Cancer J Clin 70:145–164. doi: 10.3322/caac.21601
5. Chen W, Feng P, Song X, Lv H and Lin H (2019) iRNA-m7G: Identifying N(7)-methylguanosine Sites by Fusing Multiple Features. Mol Ther Nucleic Acids 18:269–274. doi: 10.1016/j.omtn.2019.08.022
6. Furuichi Y (2015) Discovery of m(7)G-cap in eukaryotic mRNAs. Proc Jpn Acad Ser B Phys Biol Sci 91:394–409. doi: 10.2183/pjab.91.394

7. Ma J, Han H, Huang Y, Yang C, Zheng S, Cai T, Bi J, Huang X, Liu R, Huang L, Luo Y, Li W and Lin S (2021) METTL1/WDR4-mediated m(7)G tRNA modifications and m(7)G codon usage promote mRNA translation and lung cancer progression. Mol Ther 29:3422–3435. doi: 10.1016/j.ymthe.2021.08.005
8. Ying X, Liu B, Yuan Z, Huang Y, Chen C, Jiang X, Zhang H, Qi D, Yang S, Lin S, Luo J and Ji W (2021) METTL1-m(7) G-EGFR/EFEMP1 axis promotes the bladder cancer development. Clin Transl Med 11:e675. doi: 10.1002/ctm2.675
9. Chen Z, Zhu W, Zhu S, Sun K, Liao J, Liu H, Dai Z, Han H, Ren X, Yang Q, Zheng S, Peng B, Peng S, Kuang M and Lin S (2021) METTL1 promotes hepatocarcinogenesis via m(7) G tRNA modification-dependent translation control. Clin Transl Med 11:e661. doi: 10.1002/ctm2.661
10. Xia P, Zhang H, Xu K, Jiang X, Gao M, Wang G, Liu Y, Yao Y, Chen X, Ma W, Zhang Z and Yuan Y (2021) MYC-targeted WDR4 promotes proliferation, metastasis, and sorafenib resistance by inducing CCNB1 translation in hepatocellular carcinoma. Cell Death Dis 12:691. doi: 10.1038/s41419-021-03973-5
11. Rinn J and Chang H (2020) Long Noncoding RNAs: Molecular Modalities to Organismal Functions. Annual review of biochemistry 89:283–308. doi: 10.1146/annurev-biochem-062917-012708
12. Liu Y, Yang C, Zhao Y, Chi Q, Wang Z and Sun B (2019) Overexpressed methyltransferase-like 1 (METTL1) increased chemosensitivity of colon cancer cells to cisplatin by regulating miR-149-3p/S100A4/p53 axis. Aging 11:12328–12344. doi: 10.18632/aging.102575
13. Liu Y, Zhang Y, Chi Q, Wang Z and Sun B (2020) Methyltransferase-like 1 (METTL1) served as a tumor suppressor in colon cancer by activating 7-methyguanosine (m7G) regulated let-7e miRNA/HMGA2 axis. Life Sci 249:117480. doi: 10.1016/j.lfs.2020.117480
14. Subramanian A, Tamayo P, Mootha V, Mukherjee S, Ebert B, Gillette M, Paulovich A, Pomeroy S, Golub T, Lander E and Mesirov J (2005) Gene set enrichment analysis: a knowledge-based approach for interpreting genome-wide expression profiles. Proceedings of the National Academy of Sciences of the United States of America 102:15545–50. doi: 10.1073/pnas.0506580102
15. Rooney M, Shukla S, Wu C, Getz G and Hacohen N (2015) Molecular and genetic properties of tumors associated with local immune cytolytic activity. Cell 160:48–61. doi: 10.1016/j.cell.2014.12.033
16. Xu J, Ou R, Nie G, Wen J, Ling L, Mo L, Xu R, Lv M, Zhao L, Lai W and Xu Y (2022) LINC01063 functions as an oncogene in melanoma through regulation of miR-5194-mediated SOX12 expression. Melanoma research. doi: 10.1097/cmr.0000000000000803
17. Zou X, Zang Q, Zhang Z, Lu Y, Jin X and Wu Y (2021) Long noncoding RNA ARRDC1-AS1 is activated by STAT1 and exerts oncogenic properties by sponging miR-432-5p/PRMT5 axis in glioma. Biochemical and biophysical research communications 534:511–518. doi: 10.1016/j.bbrc.2020.11.051
18. Jin Y, Zhang Z, Yu Q, Zeng Z, Song H, Huang X, Kong Q, Hu H and Xia Y (2021) lncRNA ZEB1-AS1Positive Reciprocal Feedback of and α Contributes to Hypoxia-Promoted Tumorigenesis and Metastasis of Pancreatic Cancer. Frontiers in oncology 11:761979. doi: 10.3389/fonc.2021.761979

19. Zhao J, Liu J, Zhang Y, Xia Y, Du H, Yan Z, Zhou C, Xia W, Zellmer L, Liao D, Wei S and Huang H (2022) SNHG16 lncRNAs are overexpressed and may be oncogenic in human gastric cancer by regulating cell cycle progression. Neoplasma 69:49–58. doi: 10.4149/neo_2021_210518N680
20. Du T, Gao Q, Zhao Y, Gao J, Li J, Wang L, Li P, Wang Y, Du L and Wang C (2021) Long Non-coding RNA LINC02474 Affects Metastasis and Apoptosis of Colorectal Cancer by Inhibiting the Expression of GZMB. Frontiers in oncology 11:651796. doi: 10.3389/fonc.2021.651796
21. Lu B, Yin Y, Zhang Y, Guo P, Li W and Liu K (2019) Upregulation of NPL4 promotes bladder cancer cell proliferation by inhibiting DXO destabilization of cyclin D1 mRNA. Cancer cell international 19:149. doi: 10.1186/s12935-019-0874-2
22. Fang D, Peng J, Wang G, Zhou D and Geng X (2019) Upregulation of eukaryotic translation initiation factor 4E associates with a poor prognosis in gallbladder cancer and promotes cell proliferation in vitro and in vivo. International journal of molecular medicine 44:1325–1332. doi: 10.3892/ijmm.2019.4317
23. Osborne M, Volpon L, Memarpoor-Yazdi M, Pillay S, Thambipillai A, Czarnota S, Culjkovic-Kraljacic B, Trahan C, Oeffinger M, Cowling V and Borden K (2022) Identification and Characterization of the Interaction Between the Methyl-7-Guanosine Cap Maturation Enzyme RNMT and the Cap-Binding Protein eIF4E. Journal of molecular biology 434:167451. doi: 10.1016/j.jmb.2022.167451
24. Zhang H, Wang A, Tan Y, Wang S, Ma Q, Chen X and He Z (2019) NCBP1 promotes the development of lung adenocarcinoma through up-regulation of CUL4B. Journal of cellular and molecular medicine 23:6965–6977. doi: 10.1111/jcmm.14581
25. Mao L, Ling X and Chen J (2021) Cyclin H Regulates Lung Cancer Progression as a Carcinoma Inducer. Computational and mathematical methods in medicine 2021:6646077. doi: 10.1155/2021/6646077
26. Jiang Q, Zhang J, Li F, Ma X, Wu F, Miao J, Li Q, Wang X, Sun R, Yang Y, Zhao L and Huang C (2021) POLR2A Promotes the Proliferation of Gastric Cancer Cells by Advancing the Overall Cell Cycle Progression. Frontiers in genetics 12:688575. doi: 10.3389/fgene.2021.688575
27. Lone B, Ahmad F, Karna S and Pokharel Y (2020) SUPT5H Post-Transcriptional Silencing Modulates PIN1 Expression, Inhibits Tumorigenicity, and Induces Apoptosis of Human Breast Cancer Cells. Cellular physiology and biochemistry: international journal of experimental cellular physiology, biochemistry, and pharmacology 54:928–946. doi: 10.33594/000000279
28. Weng W, Yu K, Jhan J, Pang S, Chiou Y and Pang S (2022) Micro-RNA378a-3p Induces Apoptosis in Sarcomatoid Renal Cell Carcinoma and Regulates POLR2A and RUNX2 Expression. Anticancer research 42:811–825. doi: 10.21873/anticanres.15539
29. Huang J, Lo U, Wu S, Wang B, Pong R, Lai C, Lin H, He D, Hsieh J and Wu K (2019) The roles and mechanism of IFIT5 in bladder cancer epithelial-mesenchymal transition and progression. Cell death & disease 10:437. doi: 10.1038/s41419-019-1669-z
30. Deng X, Pan Y, Yang M, Liu Y and Li J (2021) PLOD3 Is Associated with Immune Cell Infiltration and Genomic Instability in Colon Adenocarcinoma. BioMed research international 2021:4714526. doi:

Figures

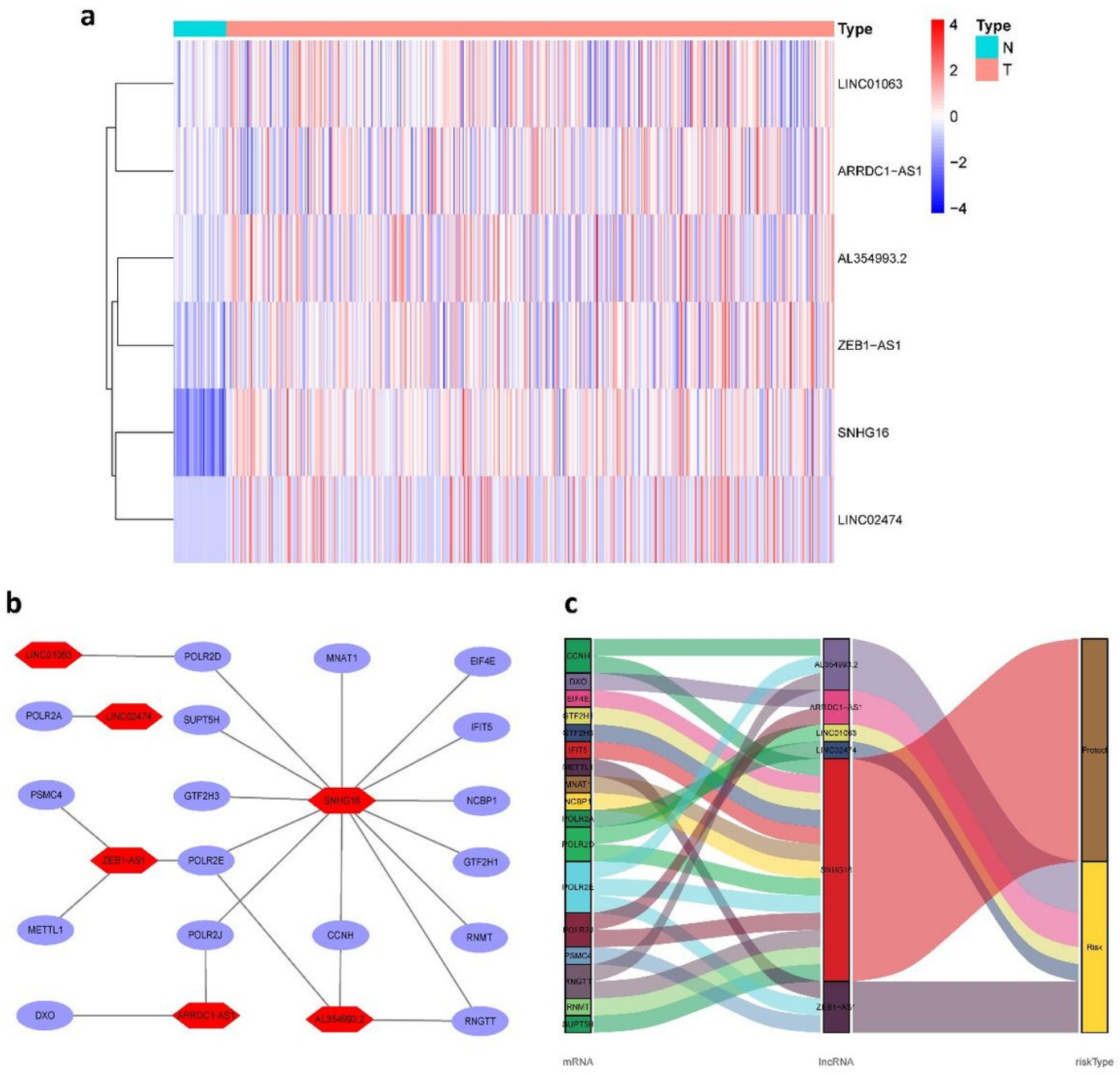

Figure 1

The expression levels and lncRNA-mRNA network of six m7G-related lncRNAs in the predictive signature. (a) The expression levels of six m7G-related lncRNAs in COAD and normal tissues. (b) The co-expression

network of prognostic m7G-related lncRNAs. (c) Sankey diagram of prognostic m7G-based lncRNAs. lncRNAs, long noncoding RNAs; COAD, Colon adenocarcinoma; N, normal; T, tumor.

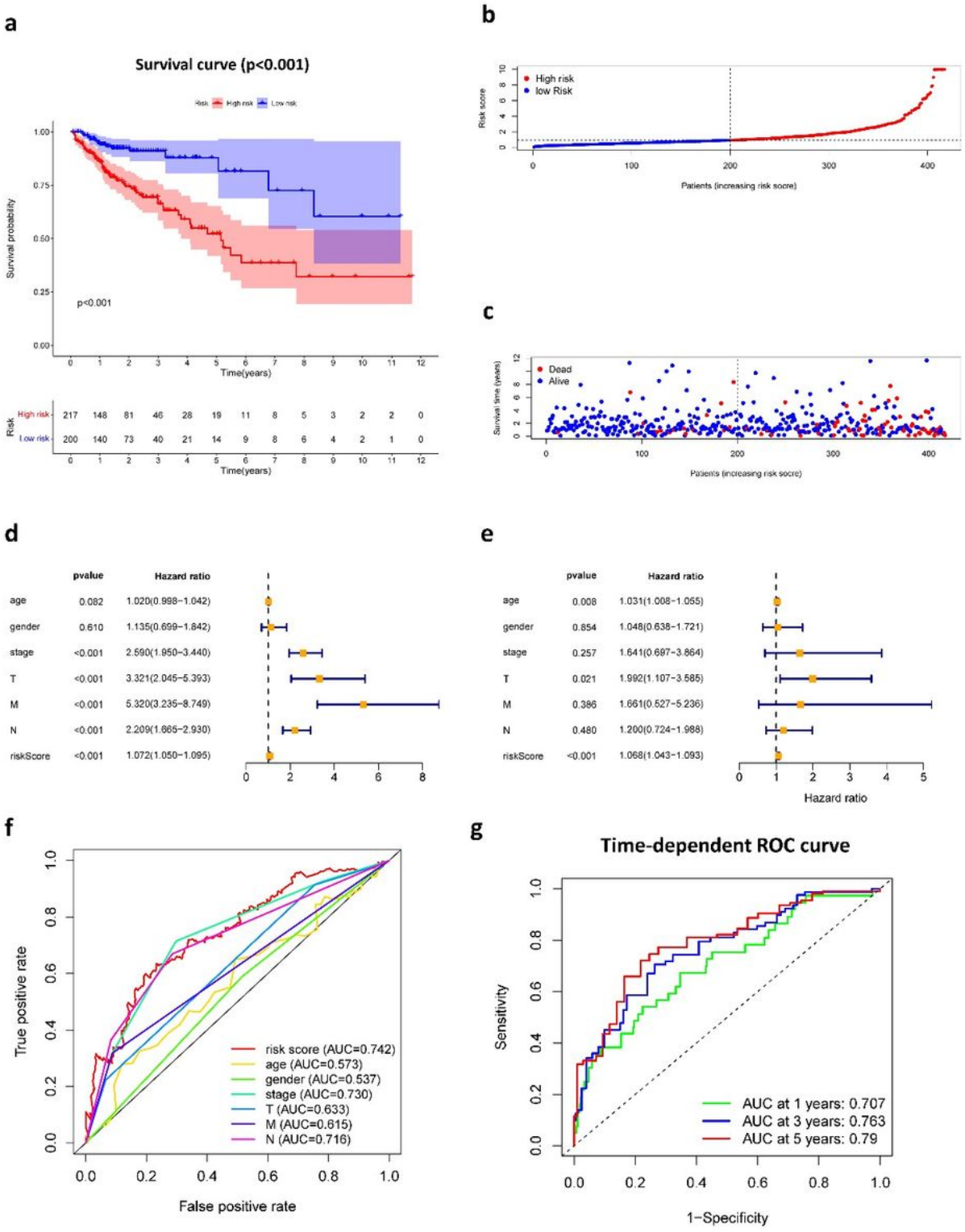

Figure 2

The correlation between the predictive signature and the prognosis of COAD patients. (a) Kaplan-Meier analysis of the OS rate of COAD patients in the high- and low-risk groups. (b) The distribution of the risk

score among COAD patients. (c) The number of dead and alive patients with different risk scores. Blue represents the number of survivors, and red represents the number of deaths. (d) Forest plot for univariate Cox regression analysis. (e) Forest plot for multivariate Cox regression analysis. (f) The ROC curve of the risk score and clinicopathological variables. (G) ROC curve and AUCs at 1-year, 3-years and 5-years survival for the predictive signature. COAD, Colon adenocarcinoma; OS, overall survival; ROC, receiver operating characteristic; AUC, area under the curve; T, tumor; N, lymph node.

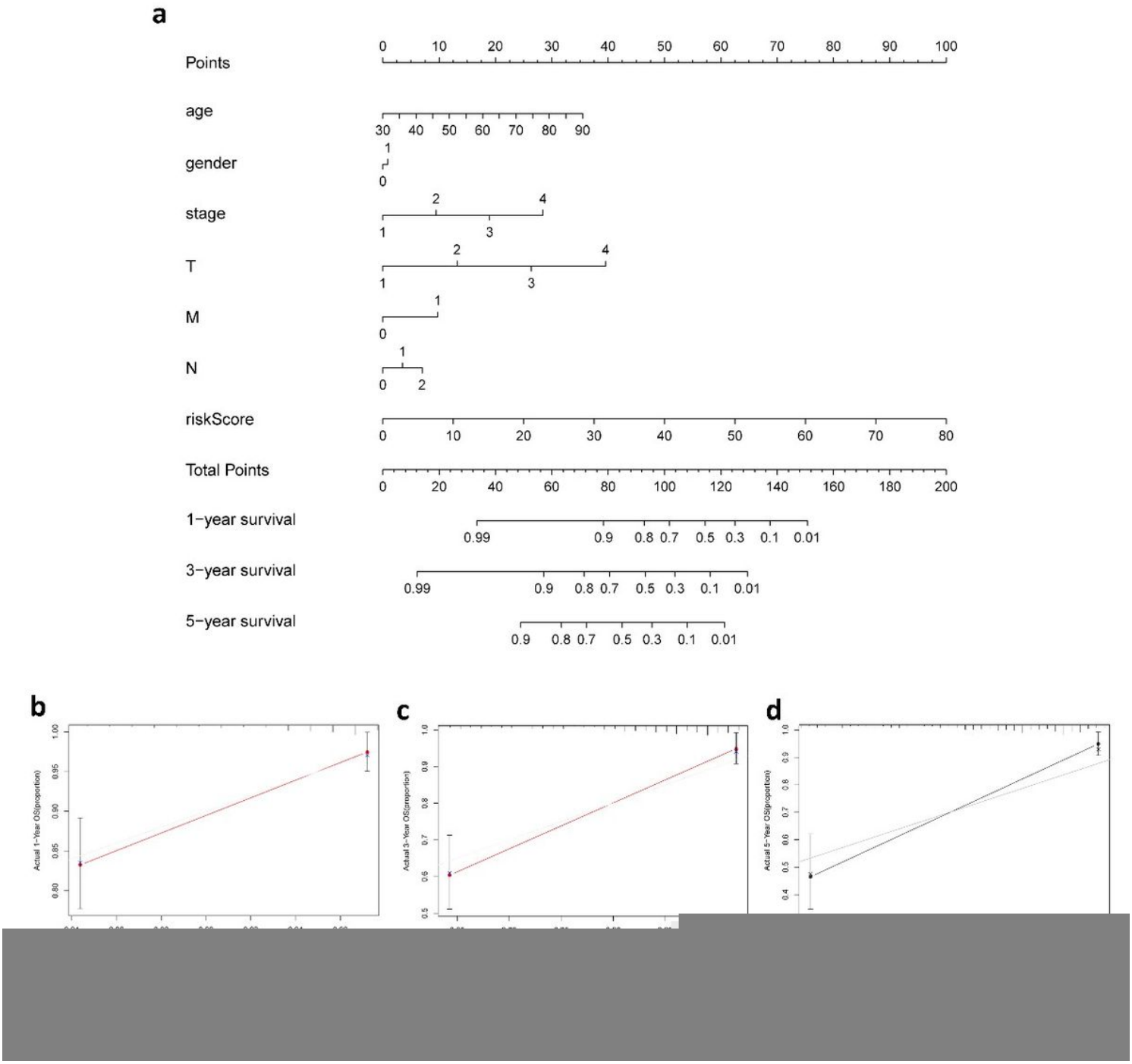

Figure 3

Construction and verification of the nomogram. (a) A nomogram combining clinicopathological variables and risk score predicts 1, 3, and 5 years OS of COAD patients. (b-d) The calibration curves test consistency between the actual OS rates and the predicted survival rates at 1, 3 and 5 years. N, lymph node; OS, overall survival; COAD, Colon adenocarcinoma.

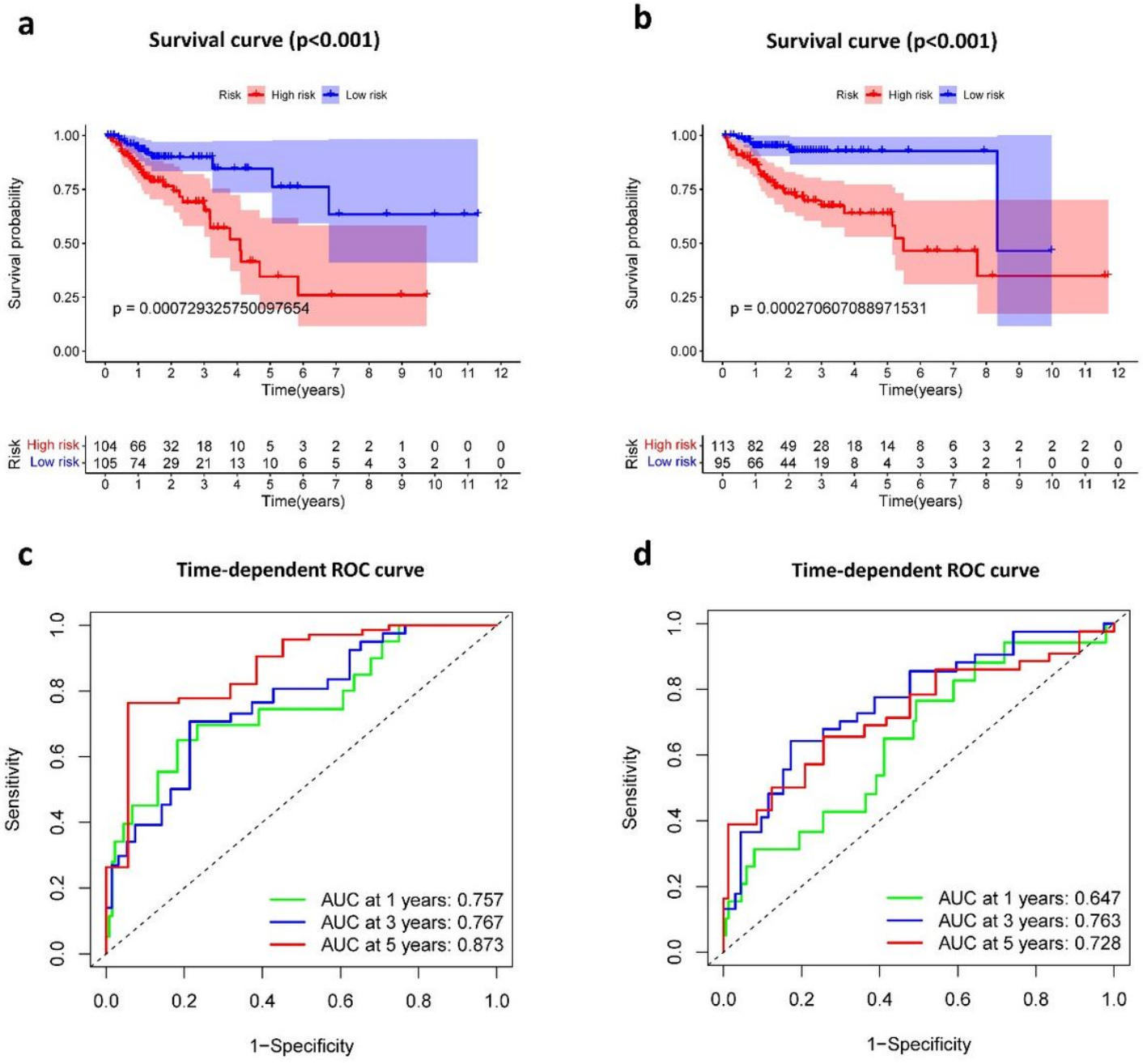

Figure 4

Internal validation of the predictive signature for OS based on the entire TCGA dataset. (a) Kaplan-Meier survival curve in the first internal cohort. (b) Kaplan-Meier survival curve in the second internal cohort. (c) ROC curve and AUCs at 1-year, 3-years and 5-years survival in the first internal cohort. (d) ROC curve and

AUCs at 1-year, 3-years and 5-years survival in the second internal cohort. ROC, receiver operating characteristic; AUC, area under the curve; OS, overall survival; TCGA, The Cancer Genome Atlas.

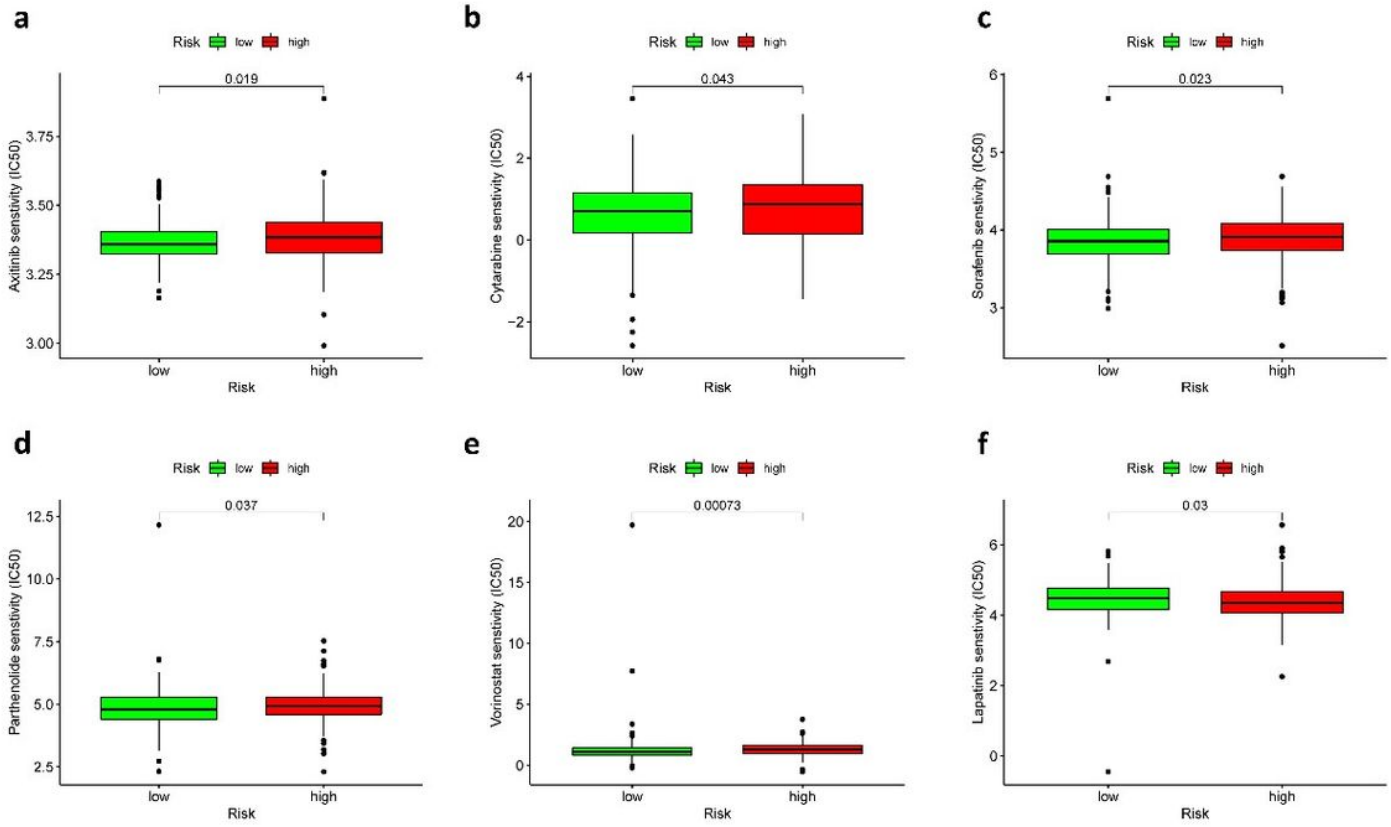

Figure 5

Comparison of treatment drugs sensitivity between high- and low-risk groups.

(a)IC50 of axitinib in high and low risk groups. (b) IC50 of cytarabine in high and low risk groups. (c) IC50 of sorafenib in high and low risk groups. (d) IC50 of parthenolide in high and low risk groups. (e) IC50 of vorinostat in high and low risk groups. (f) IC50 of lapatinib in high and low risk groups. IC50, half-maximal inhibitory concentration.

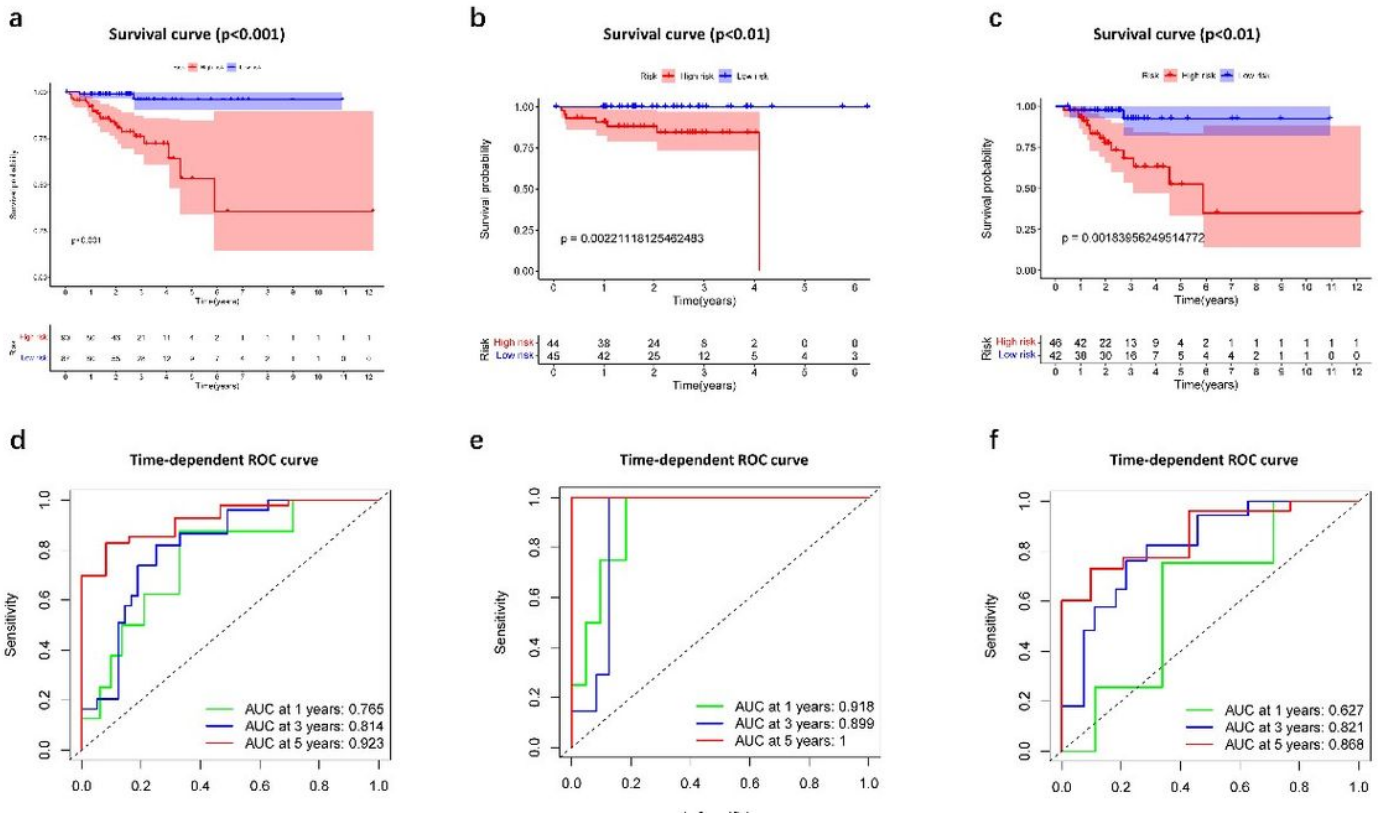

Figure 6

Evaluation of the predictive value of the ferroptosis-related lncRNA signature for DFS. (a) Kaplan-Meier survival curve in the entire dataset. (b) Kaplan- Meier survival curve in the first cohort. (c) Kaplan-Meier survival curve in the second cohort. (d) ROC curve and AUCs at 1-year, 3-years and 5-years survival in the entire dataset. (e) ROC curve and AUCs at 1-year, 3-years and 5-years survival in the first cohort. (f) ROC curve and AUCs at 1-year, 3-years and 5-years survival in the second cohort. lncRNAs, long noncoding RNAs; DFS, disease-free survival; ROC, receiver operating characteristic; AUC, area under the curve.

Supplementary Files

This is a list of supplementary files associated with this preprint. Click to download.

- 1041lncRNA.xlsx
- SupplementaryFigureS1.tif
- SupplementaryTableS1.docx